Journal of Organometallic Chemistry 694 (2009) 4178–4184

Contents lists available at ScienceDirect

Journal of Organometallic Chemistry

journal homepage: www.elsevier.com/locate/jorganchem

Dinuclear and polynuclear silver(I) saccharinate complexes with 1,3-diaminopropane and *N*-methylethylenediamine constructed from Ag···C interactions

İnci İlker [a], Okan Zafer Yeşilel [a,*], Güneş Günay [a], Orhan Büyükgüngör [b]

[a] Department of Chemistry, Faculty of Arts and Sciences, Eskişehir Osmangazi University, 26480 Eskişehir, Turkey
[b] Department of Physics, Faculty of Arts and Sciences, Ondokuz Mayıs University, 55139 Kurupelit, Samsun, Turkey

ARTICLE INFO

Article history:
Received 22 July 2009
Received in revised form 24 August 2009
Accepted 3 September 2009
Available online 11 September 2009

Keywords:
Dinuclear complex
Polynuclear complex
Ag···Ag interaction
Ag···C interaction
Saccharinate complexes
Silver(I) complexes

ABSTRACT

New dinuclear and polynuclear Ag(I) complexes with the formula of $[Ag_2(sac)_2(pen)_2]$ (**1**) and $[Ag_2(sac)_2(nmen)]_n$ (**2**), (sac = saccharinate, pen = 1,3-diaminopropane, nmen = *N*-methylethylenediamine) have been synthesized and characterized by IR spectroscopy and thermal (TG/DTG, DTA) analysis. In addition, their structures were determined by single crystal X-ray diffraction technique. In **1**, Ag(I) ions are doubly bridged by two pen ligands, besides pen ligands exhibit an interesting coordination mode by binding bridging ligand. Sac ligands connect to silver atom through its imino N atom. Furthermore, each Ag(I) ion exhibits a T-shaped coordination geometry. In **2**, Ag(I) coordination environment is again T-shaped, including weak Ag–Ag bonds. The sac exhibits bidentate bringing mode, involving its imino nitrogen and carbonyl oxygen atoms, besides, bridging of Ag(I) centres by sac ligands results in argentophilic contacts. The polymeric units are assembled into two-dimensional networks by hydrogen bonds, C–H···π stacking interactions, weak Ag···C_{sac} (η^2) and Ag···O interactions.

1. Introduction

Saccharin, alternatively named 1,2-benzisothiazoline-3-(2H) one 1,1-dioxide or *o*-sulphobenzimide in the form of its water soluble sodium salt, is widely used as a noncaloric artificial sweetener and food additive [1]. Saccharin was discovered accidentally by Fahlberg in 1878 during an investigation of the oxidation of *o*-toluenesulfonamide [2,3] and published by Remsen and Fahlberg, 1 year later [4,5]. The chemistry of saccharin had attracted attention in years past as preliminary studies showed that saccharin implanted into the bladders of mice caused urinary bladder carcinomas [6]. The ban that was consequently imposed on saccharin was lifted by the FDA in 1991 when further studies failed to form any conclusive evidence that it was a carcinogen [7]. Reports on the ability of saccharin to act as an inhibitor for certain enzyme reactions have been published [7]. Saccharin complexes have also been reported to have superoxide dismutase-like behavior (SOD) and the SOD activity of the saccharinate complexes of manganese, iron, cobalt, nickel, copper and zinc have been investigated [8,9]. The presence of several potential donor atoms such as the imino nitrogen, one carbonyl and two sulfonyl oxygen atoms makes the saccharinate anion polyfunctional ligand in coordination chemistry. Sac using these donor atoms easily exhibit mono-(N or O), bi-(N, O) or multidentate coordination types. Systematic studies and generalizations about sac have so far been undertaken. Structural data of many of sac complexes have been critically evaluated and some peculiarities regarding the geometrical characteristics of the ligand and its bond properties, discussed in detail [10]. Many studies on its metal complexes, especially those first row transition metals have been carried out [11,12]. Metal complexes of saccharin could also play an important role in understanding human metabolic processes [13]. Over the past decades, the design and synthesis of silver(I) complexes have attracted great attention because of the versatility of their coordination geometries such as linear, bent, trigonal planar, T-shaped, tetrahedral, trigonal pyramidal with diverse ligands [1–14]. This study represents the continuation of our extensive synthesis, spectral, thermal and structural characterization studies on the mixed-ligand complexes of saccharine [15,16]. Currently we determined the X-ray crystal structures of mixed-ligand saccharinato complexes of Ag(I) with 1,3-diaminopropane, $[Ag_2(sac)_2(pen)_2]$ (**1**) and *N*-methylethylenediamine, $[Ag_2(sac)_2(nmen)]_n$ (**2**) and investigated their thermal behaviors and also spectroscopic properties. It is really interesting that, the behavior of pen ligands in **1** is really different because pen ligands act as a bridging ligand. Our researches on the coordination properties of pen show that the bridging coordination mode of pen is not common. For instance, in complexes, $[Cu_2(\mu\text{-pzdc})_2(pen)_2]\cdot$

* Corresponding author.
E-mail address: yesilel@ogu.edu.tr (O.Z. Yeşilel).

0022-328X/$ - see front matter © 2009 Elsevier B.V. All rights reserved.
doi:10.1016/j.jorganchem.2009.09.009

$2H_2O$ and $[Ni(pen)_2]_5[Fe(CN)_6]_2[Fe(CN)_6]\cdot 10H_2O$, pen ligand exhibits bidentate binding mode [17,18]. Moreover, the Ag–C_{sac} bonding interactions presented for the second time, in a silver(I)-sac complex. The first Ag–C_{sac} bonding interaction was seen at $[Ag_2(sac)_2(MeCN)_2]_n$ [19]. In complex **2**, Ag–C_{sac} bonding interaction may be considered as a weak dihapto aromatic coordination between the benzene ring of sac and the silver(I) ion, anyway it's important to packing of **2** in the solid state.

2. Experimental

2.1. Materials and measurements

All reagents were purchased from commercial sources and used without any purification. IR spectra were measured on a Perkin–Elmer 100 FT-IR spectrometer using KBr pellets in the 4000–400 cm^{-1} range. Diamond TG/DTA thermal analyzer was used to

Table 1
Assignment of the most characteristic IR bands[a] of **1** and **2**.

Complexes	Assignments							
	$\upsilon(NH_2)/(NH)$	$\upsilon(CH)/(CH_2)$	$\upsilon(C{=}O)$	$\upsilon(C{-}C)$	$\upsilon_s(CNS)$	$\upsilon_{asym}(CNS)$	$\upsilon_s(SO_2)$	$\upsilon_{as}(SO_2)$
$[Ag_2(sac)_2(pen)_2]$	3267b, s	3071vw, 2930vw	1641 and 1624vs	1583 and 1459s	1332m	966s	1152vs	1258 and 1274vs
$[Ag_2(sac)_2(nmen)]_n$	3305b, s, 3078s	2922vw, 2852vw	1652 and 1625vs	1583s	1335m	967s	1121vs	1251vs

[a] Frequencies in cm^{-1}: b, broad; m, medium; vw, very weak; vs, very strong; and s, strong.

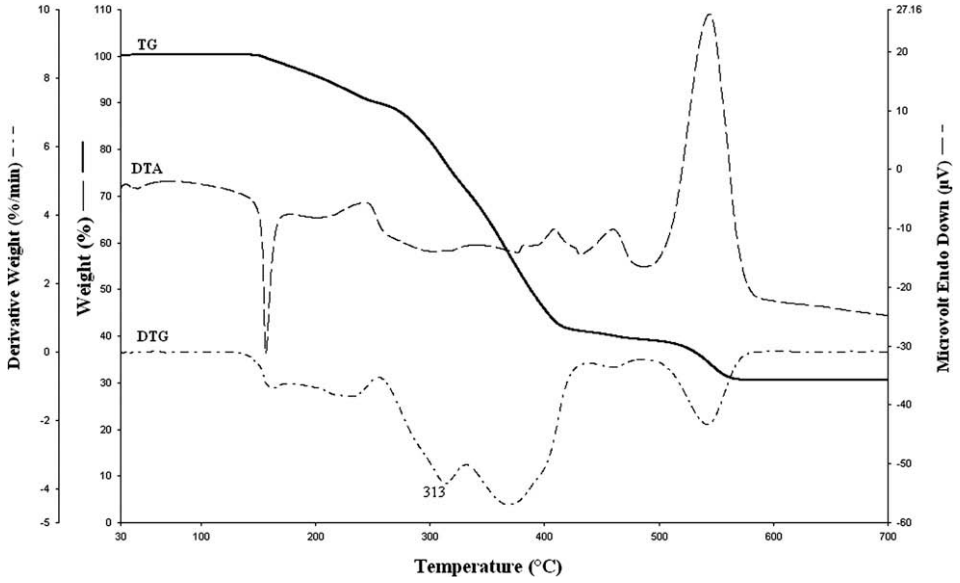

Fig. 1. TG, DTG and DTA curves of **1**.

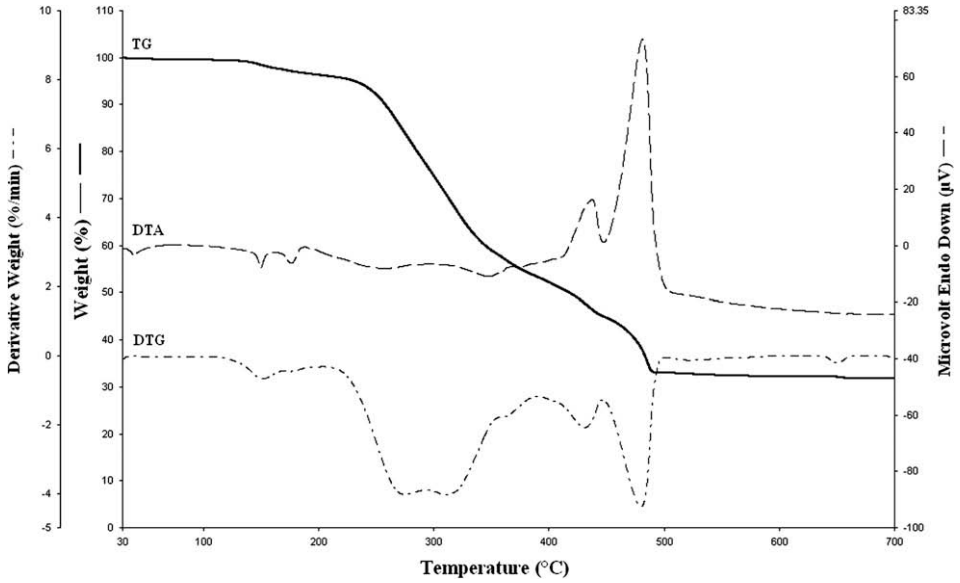

Fig. 2. TG, DTG and DTA curves of **2**.

record simultaneous TG, DTG and DTA curves in a static air atmosphere at a heating rate of 10 °C min^{-1} in the temperature range 30–700 °C using platinum crucibles.

2.2. Synthesis of *1* and *2*

$Na(Sac)_2{\cdot}H_2O$ (0.25 g, 1.22 mmol) was added to an aqueous solution (30 mL) of $AgNO_3$ (0.207 g, 1.22 mmol) with stirring at room temperature. Then, a suspension with a white precipitate formed and the addition of pen (0.090 g, 1.22 mmol) to the suspension resulted in a clear solution, which was kept in darkness at room temperature. The colorless single crystals of **1** were obtained in a week.

The preparation method used for **2** was the same as that for **1**, using the nmen ligand (0.090 g, 1.22 mmol).

2.3. Crystal structures

Diffraction experiments were carried out at 296 K on a Stoe IPDS diffractometer using Mo Kα radiation (λ = 0.71073 Å). The structures were solved by direct methods and refined using the programs SHELXS97 and SHELXL97 [20]. All non-hydrogen atoms were refined anisotropically by full-matrix least-squares methods [20]. Data collection: X-AREA, cell refinement: X-AREA, data reduction: X-RED [21]; program(s) used for molecular graphics: ORTEP-3 for Windows [22]; software used to prepare material for publication: WINGX [23].

3. Results and discussion

3.1. Synthesis

The aim of this work was to study the effects of diverse diamine derivatives as co-ligand on the coordination mode of saccharinate in mixed-ligand complexes. Previous observations showed that a second ligand in the coordination sphere of saccharinate complexes could produce N- or O- coordination of the saccharinate anion, as observed in $[Cu_2(sac)_4(Himid)_4]$, $[V(sac)_2(py)_4]$ and $[Ni(sac)_2(py)_4]$ and recently in $[Cu(sac)_2(Hpz)_4]$ [24]. The reaction of different diamine derivatives in water solution yield compounds of the formulas $[Ag_2(sac)_2(pen)_2]$ (**1**) and $[Ag_2(sac)_2(nmen)]_n$ (**2**). The composition of the complexes was determined by IR and thermal analysis in detail. Lastly, their structures were determined by single crystal X-ray diffraction technique.

3.2. IR spectra

The most significant and characteristic frequencies in the IR spectra of the complexes is shown in Table 1. The position of bands in the spectra of the complexes is similar. The IR spectra of the Ag(I) complexes exhibit the characteristic features of OH, NH_2, NH, CO, CC, symmetric and asymmetric SO_2.

For complex **1,** two characteristic $\nu(NH_2)$ stretching vibrations of 1,3-pen ligand involving hydrogen bonding could be clearly identified as strong bands in the 3270–3315 cm^{-1} range. The relatively weak bands at 2930–3071 cm^{-1} are due to $\nu(CH_2/CH)$ vibrations involving the ring H atoms. The ν(CO) bands of the sac ligands occur at 1641 and 1624 cm^{-1} as two distinct and strong bands. The absorption bands at 1583 and 1459 cm^{-1} correspond to the ring ν(CC) vibrations. The $\nu_{asym}(SO_2)$ absorption is found to split two

Table 2
Crystallographic data and structure refinement parameters for **1** and **2**.

Complexes	**1**	**2**
Empirical formula	$C_{20}H_{28}Ag_2N_6O_6S_2$	$C_{17}H_{18}Ag_2N_4O_6S_2$
Formula weight	728.34	654.21
Crystal system	Triclinic	Triclinic
Space group	$P-1$	$P-1$
a (Å)	7.9929 (4)	7.7836 (5)
b (Å)	8.8244 (5)	9.2785 (5)
c (Å)	9.6161 (5)	15.0997 (8)
α (°)	96.704 (4)	90.643 (4)
β (°)	115.014 (4)	91.384 (5)
γ (°)	90.259 (4)	106.395 (5)
V (Å^3)	609.33 (6)	1045.67 (10)
Z	1	2
μ (mm^{-1})	1.83	2.12
D_{calc} (Mg m^{-3})	1.985	2.078
Crystal size (mm)	0.58 × 0.37 × 0.19	0.38 × 0.32 × 0.25
θ Range (°)	2.33–28.10	2.29–28.05
Measured reflections	12 687	10 996
Independent reflections	2504	4334
R_{int}	0.025	0.036
$R[F^2 > 2\sigma(F^2)]$, $wR(F^2)$	0.021, 0.051	0.026, 0.073
Goodness-of-fit on F^2	1.08	1.05
$\Delta\rho_{max}$, $\Delta\rho_{min}$ (e Å^{-3})	0.27, −0.53	0.71, −0.92

Table 3
Selected bond distances (Å), angles (°) for **1**.

Bond lengths (Å)			
N1–Ag1	2.471 (2)	Ag1–N3^{i}	2.208 (2)
N2–Ag1	2.221 (2)		
Angles (°)			
N3^{i}–Ag1–N2	167.42 (7)	N2–Ag1–N1	94.82 (6)
N3^{i}–Ag1–N1	97.57 (7)		
D–H···A	H···*A* (Å)	*D*···*A* (Å)	*D*–H···*A* (°)
N2–H2A···O1^{ii}	2.40	3.185 (3)	146
N2–H2A···O1	2.62	3.269 (2)	129
N3–H3A···N1^{iii}	2.66	3.450 (3)	147
N3–H3B···O3^{i}	2.42	3.085 (2)	131

Symmetry codes: (i) $-x, -y+1, -z+1$; (ii) $x+1, -y+2, -z+1$; (iii) $x-1, y, z$; (i) $-x, -y+1, -z+1$.

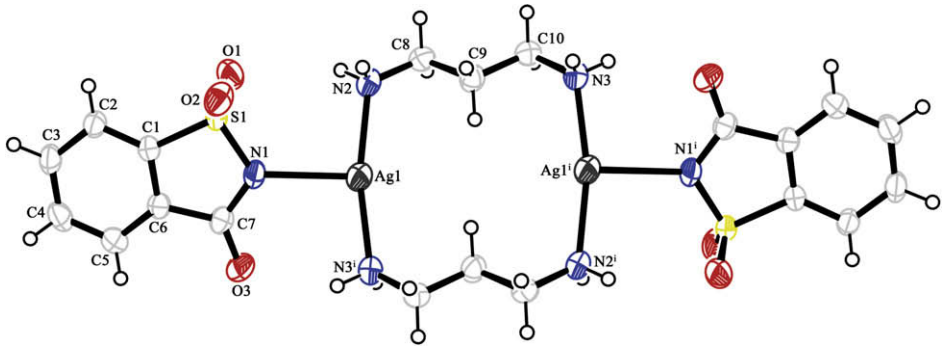

Fig. 3. The molecular structure of **1** showing the atom numbering scheme. The thermal ellipsoids are plotted at the 50% probability level.

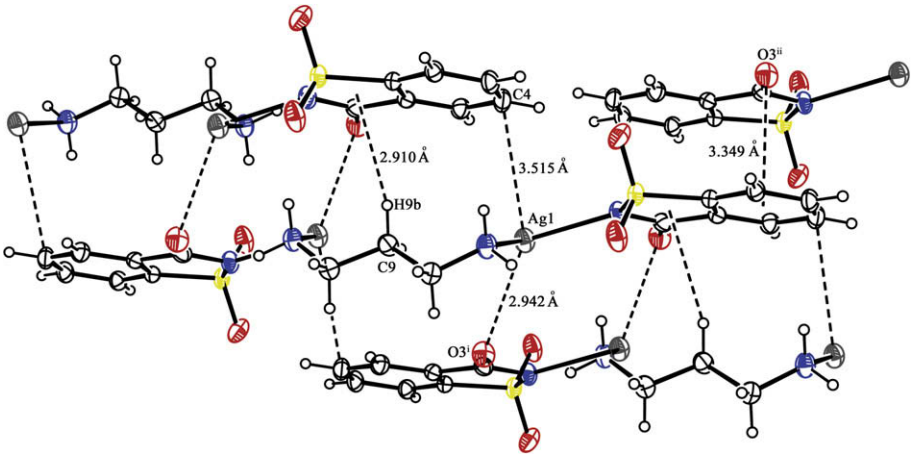

Fig. 4. The C–H···π, Ag···O and Ag···C interactions of **1**.

Table 4
Selected bond distances (Å), angles (°) for **2**.

Bond lengths (Å)			
N1–Ag2	2.169 (2)	O1–Ag1	2.255 (2)
N2–Ag1	2.175 (2)	O4–Ag2	2.294 (2)
N3–Ag1	2.350 (2)		
N4–Ag2^{i}	2.318 (2)		
Angles (°)			
N2–Ag1–O1	152.19 (7)	N1–Ag2–O4	148.56 (7)
N2–Ag1–N3	118.14 (8)	N1–Ag2–N4^{ii}	127.56 (8)
O1–Ag1–N3	89.61 (7)	O4–Ag2–N4^{ii}	82.54 (8)
D–H···A	H···*A* (Å)	*D*···*A* (Å)	*D*–H···*A* (°)
N3–H3A···O2^{iii}	2.19	2.939 (3)	139
N4–H4B···O5^{iv}	2.23	3.047 (3)	151

Symmetry codes: (i) *x*, *y* − 1, *z*; (ii) *x*, *y* + 1, *z*; (iii) *x* − 1, *y* − 1, *z*; (iv) *x* + 1, *y*, *z*.

bands at 1258 and 1274 cm^{-1}, while $\nu_{sym}(SO_2)$ band occurs as strong band at 1152 cm^{-1}. Additional peaks at 1332 and 966 cm^{-1} attributed to the symmetric and asymmetric stretching modes of the CNS moiety of sac ligands, respectively.

For complex **2,** the strong and broad absorption bands centred at 3305 and 3078 cm^{-1} are attributed to the $\nu(NH_2/NH)$ vibrations of the nmen ligand participated in hydrogen bonding. The relatively weak bands at 2922 and 2852 cm^{-1} are due to the absorption of the CH groups. The ν(CO) vibrations clearly separated as doublets at 1652 and 1625 cm^{-1}, indicating the different interactions of sac ligand. The bands with strong intensity around 1583 cm^{-1} correspond to the ν(CC) vibrations of the aromatic phenyl ring. Additional bands at 1335 and 967 cm^{-1} are assigned to the symmetric and asymmetric stretchings of the CNS moiety of the sac ligands, respectively. Very strong bands at 1251 and 1121 cm^{-1} are attributed to the stretching vibrations of $\nu_{asym}(SO_2)$ and $\nu_{sym}(SO_2)$, respectively. The *N*-coordination of the nmen ligand is confirmed by the absorption bands at around 675 cm^{-1} due to γ (py) [25].

Vibrations related to the Ag–N and Ag–O vibrations could not be identified with certainty. Also, the weak bands below 600 cm^{-1} may be attributed to both Ag–N and Ag–O vibrations.

3.3. Thermal analyzes

The TG, DTG and DTA curves show that complexes **1** and **2** exhibit a similar decomposition pathway. Both of the complexes exhibit three decomposition stages (Figs. 1 and 2) and stable up to 142 and 130 °C, respectively, above which their structures begin

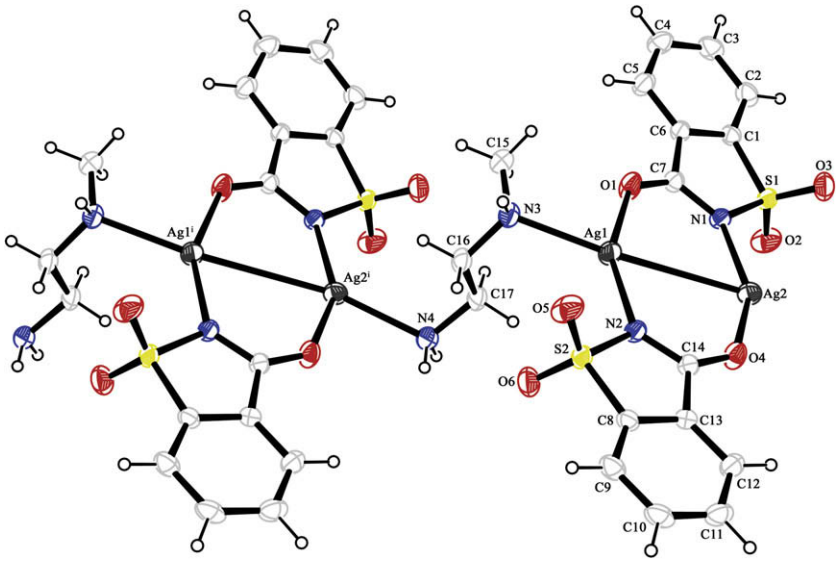

Fig. 5. The molecular structure of **2** showing the atom numbering scheme. The thermal ellipsoids are plotted at the 50% probability level.

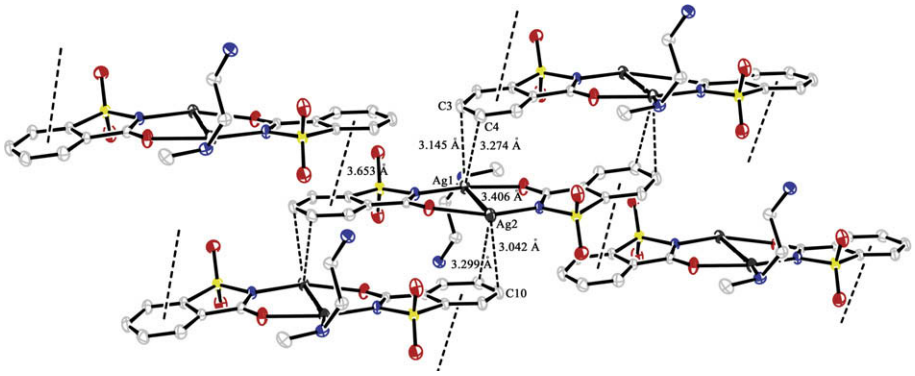

Fig. 6. The Ag···C and π···π interactions of **2**.

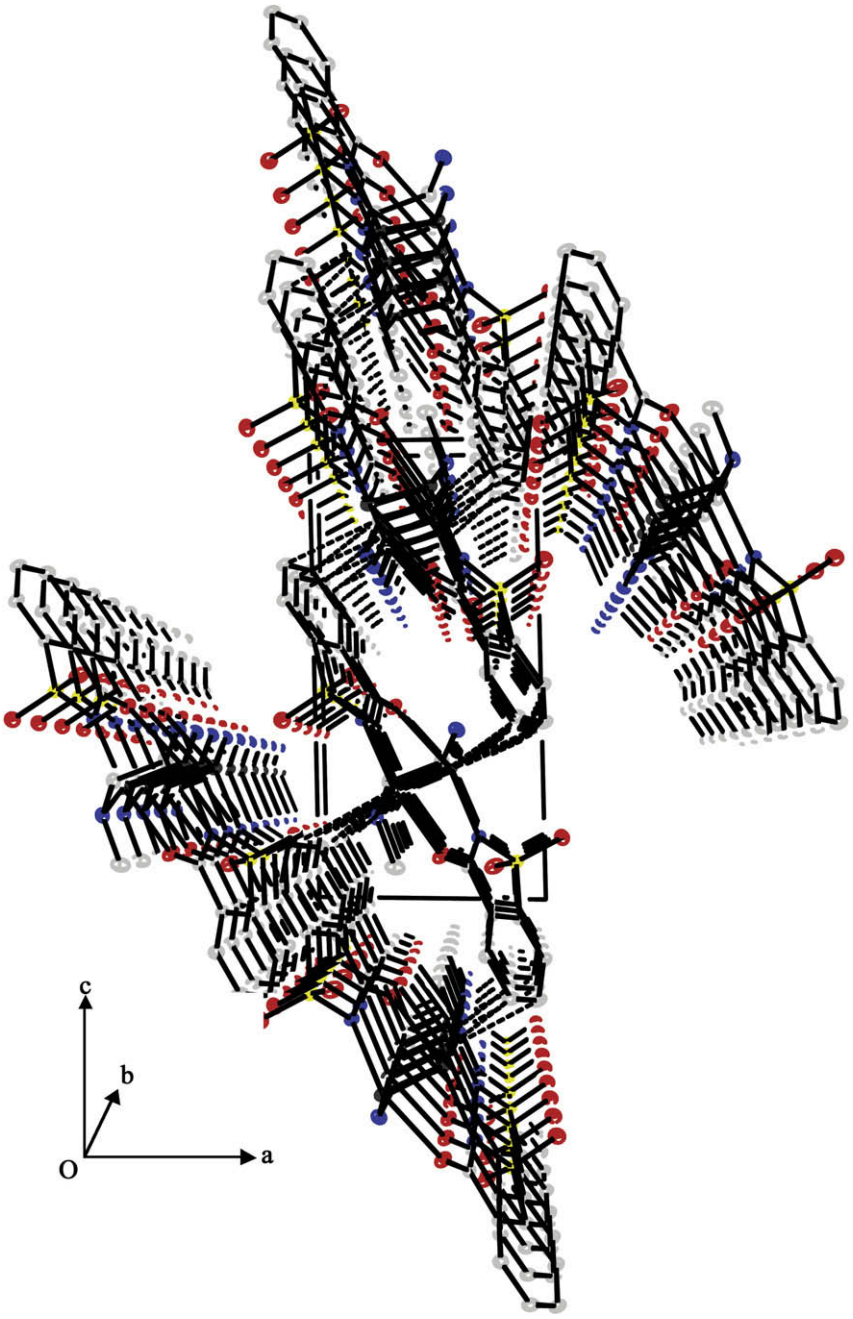

Fig. 7. Packing diagram of **2**.

to collapse. The TG curves of both **1** and **2** exhibit a continuous weight loss. Therefore, it is almost impossible to calculate mass loss values for each step for the complex **1**. However, the DTA curve displays endothermic peak at 156 °C, due to elimination of the pen ligands. For the complex **2**, endothermic removal of nmen ligand and saccharinate occurs in the temperature range of 130–354 °C with an experimental mass loss of 41.73% (Calc. 39.02%). The violently exothermic peak at 544 °C is attributed to the degradation of the sac anions for **1**, the following two stages of the temperature range of 354–503 °C, complex **2** involves the decomposition of second saccharinate ligand by the exothermic effect (DTA_{max} = 481 °C). Decomposition process both of **1** and **2** ends at around 575 °C. As well as microanalyses of the solid residues, the mass loss calculations suggest that the residue left as a final decomposition product of the complexes is metallic silver and total mass loss of (Found 69.04% and Calc. 69.91%) and (Found 67.06% and Calc. 64.27%) respectively, agrees with the propose structures well.

3.4. Crystal structures

The molecular structure of **1** with the atom labeling is shown in Fig. 3. Related crystallographic data is presented in Table 2. The selected bond lengths and angles together with hydrogen bonding geometry are collected in Table 3. The complex crystallizes in the triclinic space group $P\bar{1}$. Each silver(I) atom is coordinated by monodentate sac ligand through nitrogen atom and two bridging pen ligands, exhibiting a distorted T-shaped AgN_3 coordination environment. The Ag–N_{sac} bond distance of 2.169(2) is similar that found in the $[Ag(sac)(ppz)]_n$ (2.172(3) Å) $[Ag(sac)(bheppz)]_n$ (2.1467(15) Å) [26], $[Ag_4(sac)_4(mpyz)_2(H_2O)_2]$ (2.154(2) Å), $[Ag_2(sac)_2(pyzca)_2]_n$ (2.133(3) Å) [27], $[Ag_2(sac)_2(MeCN)_2]_n$ (2.172(2) Å) [18], but it is shorter than those reported for $[Ag_2(sac)_2(\mu\text{-aepy})_2]$ (2.449(2) Å) [28]. The Ag···Ag bond distances in the dimeric units are 5.373 Å, which are longer than the van der Waals' radius sum for silver(I) (3.44 Å), indicating the absence of any interaction between the silver(I) ions. The sac ligand is essentially planar. The individual dinuclear complexes are interconnected to each other by C–H···Cg1^{i} (2.91 Å, Cg1 = S(2)–N(1)–C(7)–C(6)–C(1), (i) = −1 + *x*, *y*, *z*), C═O···Cg2^{ii} (3.349 Å, Cg2 = C(1)–C(2)–C(3)–C(4)–C(5)–C(6), (ii) = 1 − *x*, 1 − *y*, −*z*), C═O···Ag (2.942 Å), C_{sac}···Ag (3.515 Å) interactions (Fig. 4). This is resulted in a one-dimensional chain parallel to (1 0 0) plane.

Selected bond distances and angles for **2** are listed in Table 4. In complex 2, each sac anion adopts a μ_2-bridging mode to connect with two silver ions through its imino N and carbonyl O atoms, forming dinuclear $[Ag_2(sac)_2]$ units (Fig. 5). Eight-membered bimetallic ring is formed by two silver(I) ions linked by two N–C–O bridges. The Ag(I) atom is three-coordinated by one nitrogen atom from nmen ligand, one N atom from sac ligand and one O atom from neighboring sac ligand. The coordination geometry around the silver ions is considered to be a distorted T-shaped [N2–Ag1–O1 = 152.19(7)°, N1–Ag2–O4 = 148.56(7)°, N2–Ag1–N3 = 118.14(8)°, N1–Ag2–N4^{i} = 127.56(8)° (i) = *x*, *y* + 1, *z*]. The Ag–N_{sac} bond distances [2.169(2) and 2.175(2) Å] are shorter than both the Ag–N_{nmen} bond distances [2.350(2) and 2.318(2) Å] and Ag–O_{sac} bond distances [2.255(2) and 2.294(2) Å]. These bond distances are within the normal range observed in the reported Ag(I)-sac complexes containing the N–O carbonyl bridged dimers [19,27]. The dimeric units are linked by nmen ligands, forming to a one-dimensional chain. The bridging nmen ligand is coordinated to the Ag(I) ions as a bis(monodentate) ligand *via* the nitrogen atoms. The Ag···Ag separation within the metallocycle is 3.406 Å, which are considerably less than the van der Waals' radius of silver (3.44 Å), showing a noticeable interaction between the silver(I) ions.

The molecular packing of the complex is stabilized by Cg1···Cg1^{i} [3.890, Cg = C(2)–C(3)–C(4)–C(5)–C(6)–C(7), (i) = 2 − *x*, 1 − *y*, −*z*], Cg2···Cg2^{ii} [3.651 Å, Cg = C(9)–C(10)–C(11)–C(12)–C(13)–C(14), (ii) = −*x*, 1 − *y*, 1 − *z*] and weak Ag···C [Ag(1)–C(4) = 3.274, Ag(1)–C(5) = 3.145, Ag(2)–C(11) = 3.299, Ag(2)–C(12) = 3.043, Ag(2)–C(13) = 3.293 Å] interactions between the silver(I) ion and the phenyl ring of sac (Fig. 6). This is resulted in a two-dimensional network parallel to (1 0 0) plane as illustrated in Fig. 7.

4. Conclusion

In summary, we have synthesized and structurally characterized Ag(I) complexes which derived from saccharinate and two diverse diamine ligands. One of the complexes is dinuclear and the other one is polynuclear compound and sac ligand acts as monodentate and bridging bis(monodentate) modes. In **1,** the Ag(I) atom has a T-shaped coordination geometry, determined by N atom of sac and by N atoms from two different pen ligands. Since, pen generally acts as a bidentate ligand, in that compound, the behavior of pen ligands is different by binding bridging. Complex **2** contains three-coordinated Ag(I) ions, which are linked by carbonyl O atom and imino N atom from same sac ligand, also by N atom from nmen ligand. Crystal structures are stabilized by intra- and intermolecular O–H···O hydrogen bonds and π···π interactions and Ag···C interactions.

Appendix A. Supplementary data

CCDC 728981 and 728982 contain the supplementary crystallographic data for complexes **1** and **2**. These data can be obtained free of charge via http://www.ccdc.cam.ac.uk/conts/retrieving.html, or from the Cambridge Crystallographic Data Centre, 12 Union Road, Cambridge CB2 1EZ, UK; fax: (+44) 1223-336-033; or e-mail: deposit@ccdc.cam.ac.uk. Supplementary data associated with this article can be found, in the online version, at doi:10.1016/j.jorganchem.2009.09.009.

References

[1] V.T. Yilmaz, S. Hamamci, W.T.A. Harrison, C. Thone, Polyhedron 24 (2005) 693.
[2] B. Schulze, K. Illgen, J. Prakt. Chem. 339 (1997) 1.
[3] J.W. Ellis, J. Chem. Educ. 72 (1995) 671.
[4] I. Remsen, C. Fahlberg, Ber. Dtsch. Chem. Ges. 12 (1879) 469.
[5] I. Remsen, C. Fahlberg, J. Am. Chem. Soc. 1 (1879/1880) 426.
[6] M.J. Allen, E. Bayland, C.E. Dukes, E.S. Horning, J.G. Watson, Brit. J. Cancer 11 (1975) 212.
[7] C.T. Supuran, M.D. Banciu, Rev. Roum. Chim. 36 (1991) 1345.
[8] T. Mann, D. Keilin, Proc. Royal Soc. (Lond.) B 126 (1938) 303.
[9] M.C. Apella, R. Totaro, E.J. Baran, Biol. Trace Elem. Res. 37 (1993) 293.
[10] E.J. Baran, V.T. Yilmaz, Coord. Chem. Rev. 250 (2006) 1980.
[11] B. Kamenar, G. Jovanovski, Cryst. Struct. Commun. 11 (1982) 257.
[12] F.A. Cotton, G.E. Lewis, C.A. Murillo, W. Schwotzer, G. Valle, Inorg. Chem. 23 (1984) 4038.
[13] S.Z. Haider, K.M.A. Malik, K.J. Ahmed, H. Hess, H. Riffel, M.B. Hursthouse, Inorg. Chim. Acta 72 (1983) 21.
[14] V. McKee, J. Nelson, D.J. Speed, R.M. Town, J. Chem. Soc., Dalton Trans. (2001) 3641.
[15] O.Z. Yesilel, C. Darcan, E. Sahin, Polyhedron 27 (2008) 905.
[16] O.Z. Yesilel, H. İçbudak, H. Ölmez, P. Naumov, Synth. React. Inorg. Metal 33 (2003) 77.
[17] O.Z. Yesilel, A. Mutlu, O. Büyükgüngör, Polyhedron 28 (2009) 437.
[18] S.Z. Zhan, K.B. Yu, J. Liu, Inorg. Chem. Commun. 9 (2006) 1007.
[19] V.T. Yilmaz, S. Hamamci, C. Kazak, J. Organomet. Chem. 693 (2008) 3885.
[20] G.M. Sheldrick, SHELXS-97 and SHELXL-97. Program for Refinement of Crystal Structures, University of Göttingen, Germany, 1997.
[21] Stoe&Cie, X-Area (Version 1.18) and X-Red32 (Version 1.04), Stoe&Cie, Darmstadt, Germany, 2001/2002.
[22] L.J. Farrugia, J. Appl. Crystallogr. 30 (1997) 565.
[23] L.J. Farrugia, J. Appl. Crystallogr. 32 (1999) 837.
[24] P. Naumov, G. Jovanosvski, M.G.B. Drew, S.W. Ng, Inorg. Chim. Acta 314 (2001) 154.

[25] K. Nakamoto, Infrared and Raman Spectra of Inorganic and Coordination Compounds, fifth ed., Wiley Interscience, New York, 1997. pp. 59–62.
[26] V.T. Yilmaz, S. Hamamci, O. Büyükgüngör, Polyhedron 27 (2008) 1761.
[27] V.T. Yilmaz, E. Senel, E. Guney, C. Kazak, Inorg. Chem. Commun. 11 (2008) 1330.
[28] S. Hamamci, V.T. Yilmaz, W.T.A Harrison, Z. Naturforsch. 60 (2005) 978.